Applied Surface Science 259 (2012) 542–546

Contents lists available at SciVerse ScienceDirect

Applied Surface Science

journal homepage: www.elsevier.com/locate/apsusc

Self-supporting superhydrophobic thin polymer sheets that mimic the nature's petal effect

Mustafa Karaman[a,b,*], Nihat Çabuk[a], Demet Özyurt[a], Özcan Köysüren[a,b]

[a] Department of Chemical Engineering, Selcuk University, 42031, Konya, Turkey
[b] Advanced Technology Research and Application Center, Selcuk University, 42031, Konya, Turkey

ARTICLE INFO

Article history:
Received 10 February 2012
Received in revised form 8 July 2012
Accepted 11 July 2012
Available online 22 July 2012

Keywords:
Petal effect
iCVD
Biomimetics
Bioreplication
Contact angle

ABSTRACT

The high adhesive force between the red rose petal and the water droplet on its surface is termed as the 'petal effect', which is caused by the hierarchical array of micro papilla on the surfaces together with the nano-folds existing on top of each papilla. Because of that special surface topography, the surface is superhydrophobic, but at the same time highly adherent to the water droplet such that the droplet cannot move even if the surface is turned upside down. In this work, we produced a thin (thickness below 1 μm) self-supporting polymer sheet that mimics the surface of a red rose petal. The product is a two-layer polymer sheet made from poly(glycidyl methacrylate) (PGMA) as the supporting layer and a hydrophobic poly(1H,1H,2H,2H-perfluorodecyl acrylate) (PPFDA) on top of it as the functional layer, both of which were deposited by initiated chemical vapor deposition (iCVD) process. The integration of conformal and solvent-free iCVD process into the classical two-step molding procedure allowed exact transfer of surface topography of the petal surface, which was verified by SEM analysis. The static contact angle of water droplet on the surface of the polymer replica was found to be $152 \pm 3^{\circ}$, and the water droplet did not roll-off even the polymer sheet is tilted or turned upside down.

1. Introduction

Many of the biological surfaces in nature have unique properties due to their well-organized surface structures. For example, many plant leaves exhibit excellent self-cleaning characteristics [1–3]. Water droplets on a lotus leaf cannot stay on the surface and roll off quickly with very small inclinations, removing the dirt on the surface. The roughness caused by the hierarchical micro and nano structures throughout the surface together with the low surface energy wax is the reason behind the superhydrophobic behavior of the lotus leaves [4,5]. Such useful properties caused by the natural orientation of the living surfaces inspired many scientists to develop similar artificial surfaces with superior capabilities. The petal surfaces of red rose exhibit a superhydrophobic behavior (water contact angle greater than 150°) with a difference in their contact angle hysteresis with respect to the behavior of lotus leaves. Their surfaces are so adhesive to the water droplets that, even if they are turned upside down, water droplets remain attached to their surfaces for very long times. This phenomenon is known as rose petal effect, and it is caused by the array of micro papilla on the surfaces of the petal together with the nano folds existing on each papilla top [6]. These hierarchical micro and nano structures provide sufficient roughness for superhydrophobicity but have high adhesive force with water. Biomimetics is termed as the applications of biological systems found in nature to design engineering materials having special functionalities. Artificially prepared surfaces having special wettability and functionalities that were inspired from plant leaves have been the subject of many academic studies [7–9]. The main route to achieve such hydrophobic surfaces involves the creation of surface roughness caused by the macro and nano domains out of low surface energy materials [10–13]. Template assisted methods are based on the formation of organic or inorganic materials over rough templates which are later removed or peeled-off to obtain self-standing replicas [14,15]. Replica formation techniques involve atomic layer deposition, nano casting, chemical vapor deposition and physical vapor deposition (PVD). The desirable method for replication of a natural surface functionality should reproduce the surface topography with high accuracy, while producing replicated surfaces with controllable chemistries. A special CVD technique, called initiated chemical vapor deposition (iCVD) is capable of forming thin polymeric layers over complex substrates [16]. In iCVD, resistively heated filaments above the substrate provide the energy for reaction; therefore the substrate to be coated remains free from solvents, high temperatures, plasma or light sources, which can alter the chemical and/or physical nature of the fragile substrates [17]. Also, the conformal nature of the iCVD process allows uniform coatings around

* Corresponding author at: Department of Chemical Engineering, Selcuk University, 42031, Konya, Turkey. Tel.: +90 332 223 1972; fax: +90 332 241 0635.
E-mail address: karamanm@selcuk.edu.tr (M. Karaman).

0169-4332/$ – see front matter © 2012 Elsevier B.V. All rights reserved.
http://dx.doi.org/10.1016/j.apsusc.2012.07.079

substrates having complicated geometries. For these reasons, iCVD is considered to be ideal method for biomimetic studies.

In this work, we used initiated chemical vapor deposition (iCVD) method, for the first time, to form polymeric duplicates of rose petal structures. First, the patterns on the petal surfaces were copied on a poly vinyl alcohol mold. The ability of iCVD to form functional polymer films on fragile polymer surfaces like PVA mold allowed the exact replication of nano and micro structures on the mold surfaces.

2. Experimental

2.1. Materials

PVA was purchased from Sigma–Aldrich (Mw = 13,000–23,000). The monomers glycidyl methacrylate (97%, Aldrich) and 1H,1H,2H,2H-perfluorodecyl acrylate (97%, Aldrich), and the initiator tert-butyl peroxide (TBPO, 98%, Aldrich) were used as received.

2.2. Negative mold preparation from rose petal

6 wt% poly vinyl alcohol (PVA)–water solution was poured on the surface of a red rose petal. After waiting 24 h at ambient conditions to evaporate all of the water, the remaining PVA thin film on the petal surface was peeled off. The obtained PVA film has inverse petal structures on the surface and was used as a mold during the iCVD process.

2.3. iCVD of polymeric duplicate films on PVA mold surface

Polymer films were deposited on PVA molds in a custom built vacuum reactor (Fig. 2b). The substrates were placed on a water circulated cooling plate in the reactor. Resistively heated 14 tungsten filaments (Alfa Aesar) placed 2 cm above the substrate surface provide energy to thermally decompose the reactants. Monomers GMA and PFDA were vaporized in separate stainless steel jars kept at 65 °C and 80 °C, respectively. The initiator TBPO was vaporized in a glass jar at room temperature. Flow rates of monomers were adjusted by needle valves, whereas the flow rate of initiator was adjusted by a mass flow controller (MKS). The pressure in the reactor was controlled by a downstream pressure controller (MKS) equipped with a Baratron vacuum gauge (MKS). Vacuum was created by a rotary vane vacuum pump (Edwards RV8). The process conditions for successive depositions are given in Table 1. Real-time control of the film thicknesses during the depositions were performed using a laser interferometer equipped with a 633 nm He–Ne laser source and a laser power meter. Thickness measurements were made using reflections off a reference silicon wafer. After depositing thin polymer films on PVA surfaces, the products were washed with distilled water carefully to remove the entire PVA mold. Finally, remaining thin polymer sheets were transferred to glass slides for characterizations.

Table 1
Deposition conditions.

PGMA deposition		PPFDA deposition	
$T_{substrate}$ (°C)	25	$T_{substrate}$ (°C)	35
$T_{filament}$ (°C)	220	$T_{filament}$ (°C)	250
$P_{reactor}$ (mTorr)	350	$P_{reactor}$ (mTorr)	100
FR_{GMA} (sccm)	1	FR_{PFDA} (sccm)	0.6
FR_{TBPO} (sccm)	0.5	FR_{TBPO} (sccm)	0.1
Deposition time (min)	30	Deposition time (min)	5

2.4. Characterization

Scanning electron microscopy (SEM) (Zeiss LS-10) was used to analyze the surfaces of polymer replicas and dried rose petals. The surface of the fresh rose petal was monitored by an environmental scanning electron microscope (ESEM) (FEI Quanta 200 FEG). Contact angle measurements were carried out on a Kruss Easy Drop contact angle measurement system at ambient temperature using distilled water as the measurement liquid. The average contact angle on a surface was obtained by measuring at five different positions of the same sample. Chemical characterization of the films was carried out by FTIR (Nicolet i10) spectrophotometer.

3. Results and discussion

Fig. 1 shows ESEM and SEM images of the fresh and dry red rose petal surfaces, respectively. The surface of the fresh petal is covered by papillae that have unique semi-spherical shapes. The top of each papilla contains nano folds heading toward the center. These structures on the rose petal surface allows for hydrophobicity, with a measured static contact angle of around 151 ± 3°. Because of a large adhesive force between the water droplet and the rose petal surface, 5 μL water droplets on the petal surfaces cannot be moved

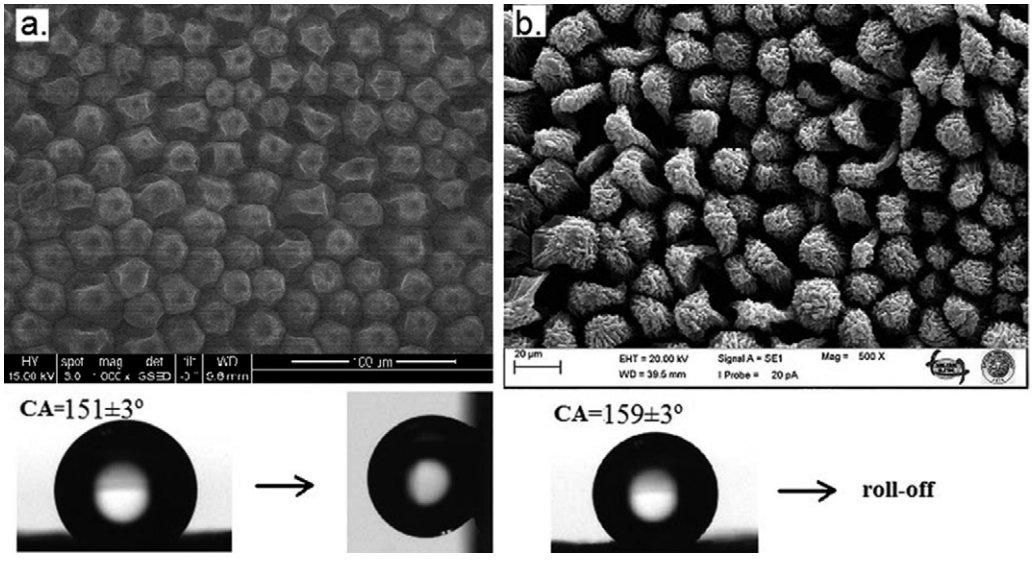

Fig. 1. SEM figures of: (a) fresh and (b) dry rose petal surfaces. Below the figures are the photographs of 5 μL water droplets over the flat (left) and 90° tilted (right) surfaces.

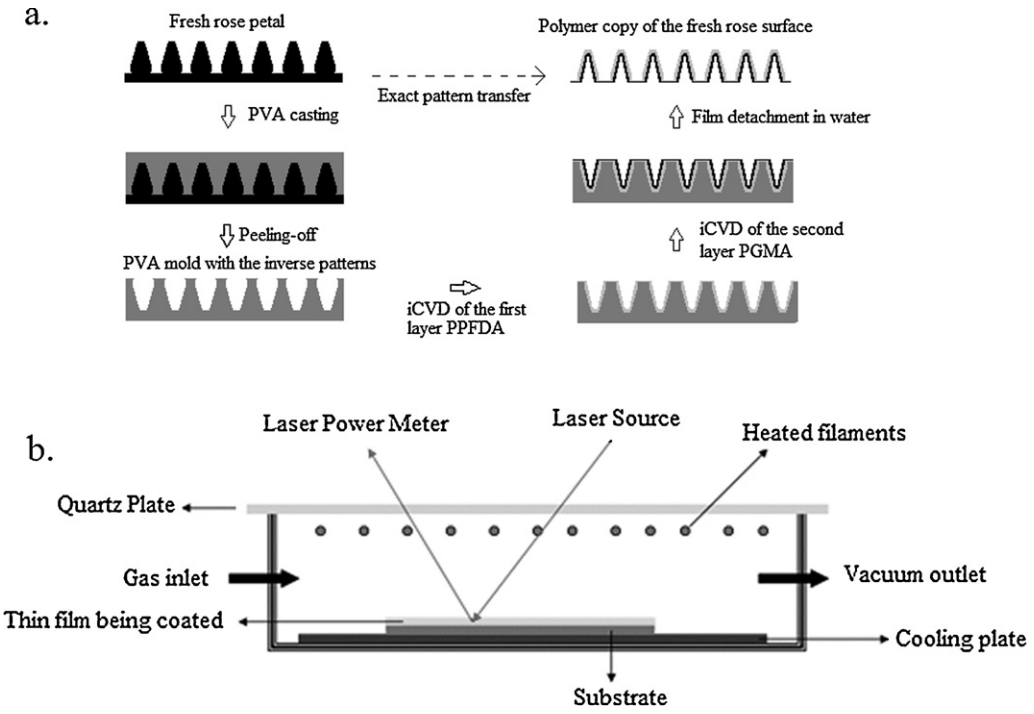

Fig. 2. Schematic representation of: (a) duplication process and (b) iCVD reactor.

even if the surface is tilted to 90° or turned upside down. The dry rose petal surface, on the other hand, shows a contact angle of as high as $159 \pm 3°$, and the contact angle hysteresis is quite low so that the droplet started to move even with small inclination of the surface. This behavior of the dry rose petal is quite similar to the wetting behavior of water droplet on lotus leafs, where the papillae have smaller diameters with varying heights, and uniformly distributed low surface energy wax tubules cover the whole surface [18]. Because of that unique structure, the lotus surfaces are not only super hydrophobic but also self-cleaning with very low contact angle hysteresis. The static contact angle value on lotus surface is around 163° [1]. Similar to the lotus effect, water droplets are in minimal contact with the surface of dry rose petal, and air is trapped between the shrunken papillae and water surface; which can be explained by Cassie wetting state [19]. In the Cassie State, water does not wet the surface and is easily roll-off over the trapped air which acts as a cushion between the surface micro domains. In the case of the fresh rose, the area between the papillae surfaces is wetted by water, making the adhesive force between the water and solid surface very high. This wetting behavior was recently termed as the 'Cassie Impregnating State' [6]. In that state, the nano-sized grooves between the nano-folds existing on top of each papilla cannot be wetted, which cause the observed superhydrophobicity.

In the bionic duplication process, first a poly vinyl alcohol mold that has negative patterns was fabricated by solution casting method. The schematic representation of duplication steps is given in Fig. 2a. The wetting behavior of the rose petal surfaces allowed water solution to penetrate deep into the papillae, allowing an exact transfer of surface shapes to the PVA mold. This is clearly seen in Fig. 3a. The same procedure was not applicable to the dry rose surfaces where water cannot penetrate into the grooves. In the second step, the inner surface of the polymer mold is coated by the polymer films using the iCVD set-up (Fig. 2b). First layer that is in contact with the inner mold surface is an ultra-thin (less than 50 nm) PPFDA film. Because of its high fluorine content and $-CF_3$ terminated side group, PPFDA is a low-surface energy material. iCVD deposited PPFDA thin film on polished silicon wafer showed static contact angle value of $117 \pm 3°$. Because of the extremely smooth nature of the deposits on polished silicon surfaces, that CA value can be attributed completely to the surface chemistry of the material.

Fig. 4 shows the FTIR spectra of the iCVD deposited PPFDA and PGMA films. Both spectra contain a sharp peak at 1741 cm^{-1} caused by C=O stretching. Besides, the absence of absorption bands around 1560 cm^{-1} proves that the polymerization proceeded through unsaturated vinyl bonds. In the spectrum of PPFDA, the sharp peaks at 1203 cm^{-1} and 1153 cm^{-1} belong to $-CF_2-$ stretching

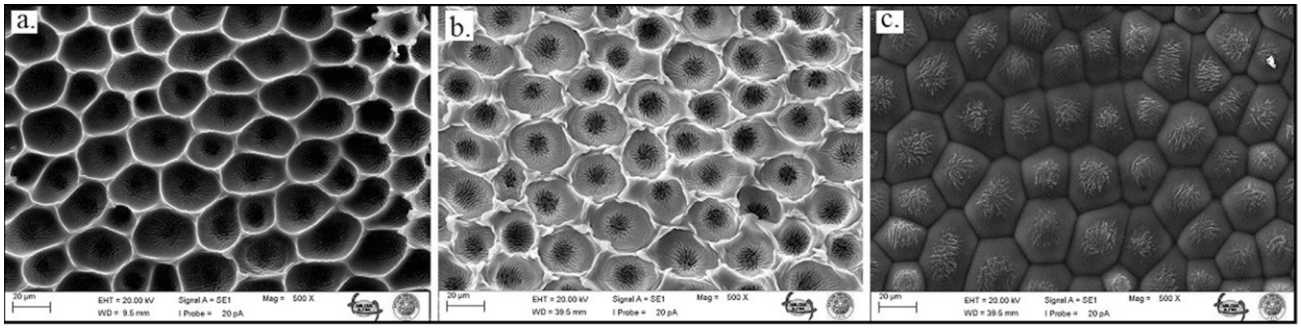

Fig. 3. SEM images of the top surfaces of: (a) PVA mold with a negative pattern; (b) iCVD coated PVA mold and (c) polymer replica.

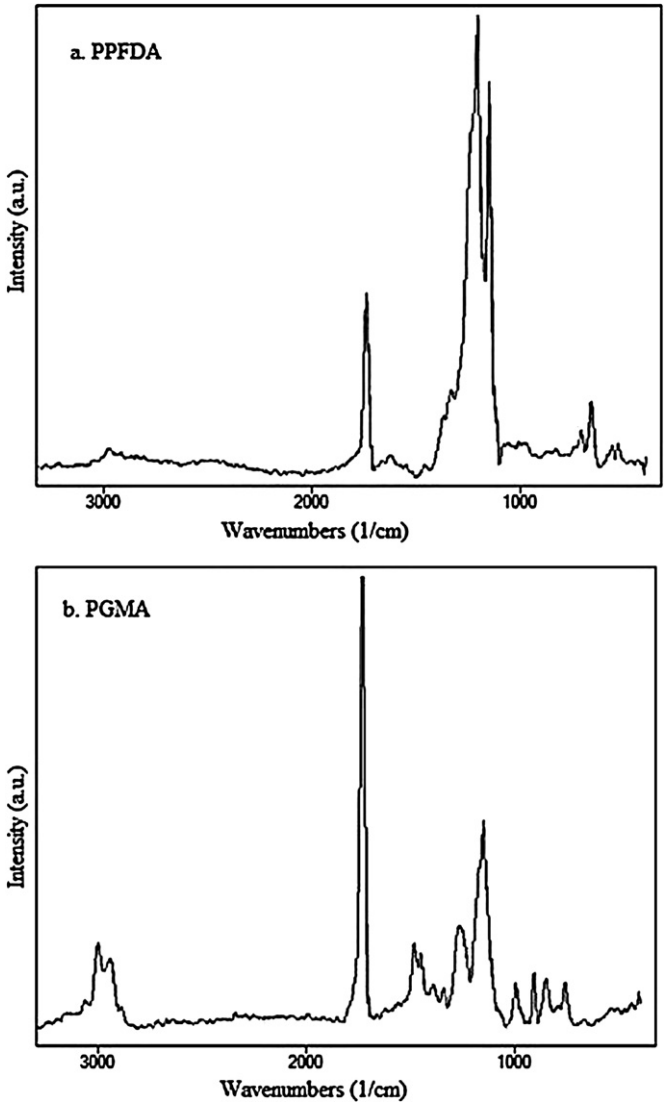

Fig. 4. FTIR Spectra of iCVD deposited: (a) PPFDA and (b) PGMA films.

and $-CF_2-CF_3$ end group, respectively. The characteristic peaks belonging to the pendent epoxide group at 907 cm^{-1}, 848 cm^{-1}, and 760 cm^{-1} were all clearly resolved from the spectrum of PGMA. In both spectra, the peaks belonging to the functional groups could be distinctly resolved as they are sharp and narrow, which implies the capability of iCVD to produce chemically well-defined polymer films.

Fig. 3b shows the ability of iCVD process to conformally coat the inner surfaces of the polymer mold. The micro and nano scale features on the inner surfaces of the PVA mold is exactly repeated by the iCVD deposited polymer films. In the conventional wet processes involving polymer casting on mold surfaces, the surface tension of fluids and solvent related compatibility problems usually lowers the quality of the transferred patterns from mold to the polymer replicas. Besides, the solvent related damages on the surface may ruin the surface topographies. In a dry process like iCVD, the problems caused by wet solvents are eliminated. Also, being a bottom-up process, iCVD produces polymers starting from monomers, therefore a desired surface chemistry can easily be implemented on a specially roughened surface by a careful choice of the starting monomers. After the film deposition process, PVA mold was dissolved in water, and Fig. 3c shows the top view of the remaining replica film, which is a perfect copy of the fresh red rose surface. That film was successfully transferred from the water solution in a beaker onto glass slides without introducing any defect. Fig. 5 shows a cross-sectional view of the self-supporting PGMA–PPFDA film with surface topography exactly the same as the fresh rose petal surfaces, with a film thickness of 430 nm, which was estimated from the SEM image of Fig. 5c. Also, the back-side of the film was observed to be as uniform as the front side with negative patterns covering the whole surface (Fig. 5b). Therefore, SEM analyses confirmed the production of a two layer polymer film with a thickness below 500 nm, with a surface topography exactly the same as the parent biological surface. Static contact angle of 5 μL water droplets on the surface of the self-supporting replica sheet was $152 \pm 3^{\circ}$, which is very close to the CA value observed for real petal surfaces. Besides, replica surface shows a very high contact angle hysterysis. 10 μL droplets placed on the replica surfaces did not roll off when the film is tilted perpendicularly or turned upside down.

The effect of water droplet evaporation on contact angle is another useful way to investigate the wetting behaviors of surfaces [20,21]. The similarity of the wetting behavior between the real petal and replica surfaces were further investigated by evaporating 7 μL droplets on both surfaces. Fig. 6 shows the static contact angle changes on both surfaces with decreasing droplet sizes during evaporation. In both surfaces droplets were evaporated and collapsed within less than 40 min. The changes in both surfaces are very similar indicating again the similarities between the surfaces. The contact angles of the droplets on both surfaces were seen to steadily decrease over time with decreasing droplet volume. Because of the high adhesion force between the surfaces and the water droplet, contact diameter at the solid liquid interface remains relatively unchanged during evaporation; however droplet volume decreases continuously. Therefore, it is expected that contact angle value should decrease with time during the evaporation. In real and replica surfaces, exactly the same behaviors were observed which

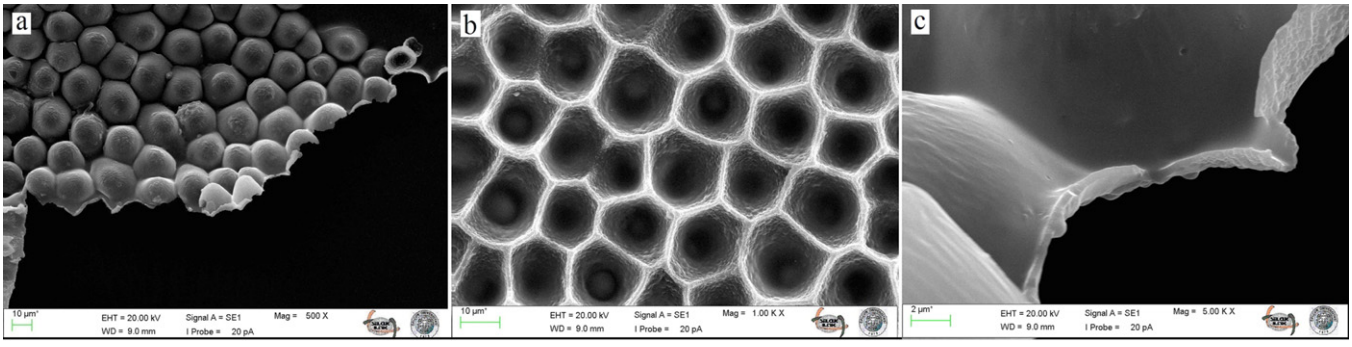

Fig. 5. Cross-sectional SEM images of the polymer replica sheet at: (a) 500×, (b) 1000× and (c) 5000× magnifications.

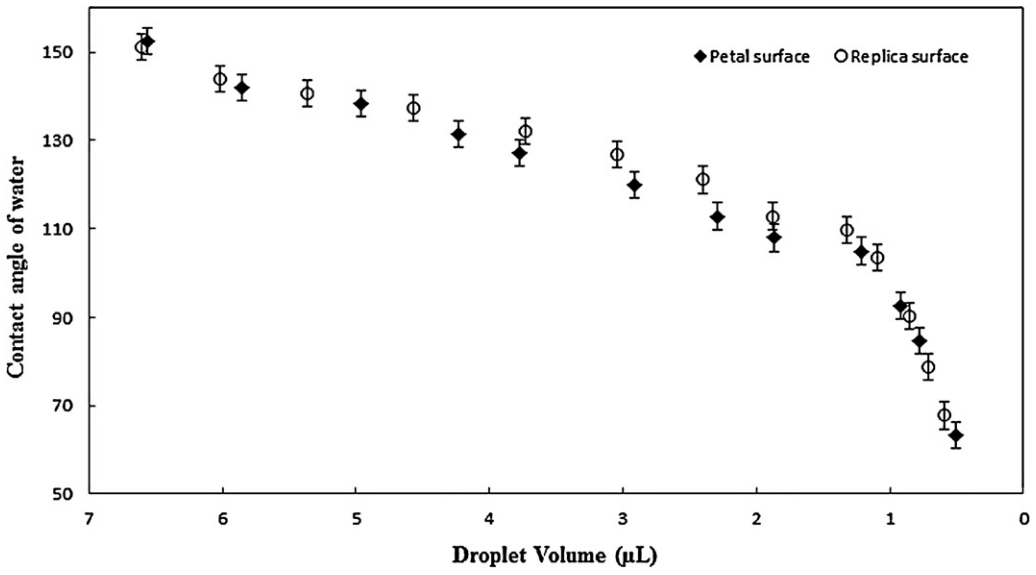

Fig. 6. Contact angle changes of evaporating water droplets on the real fresh petal and replica sheet surfaces.

further verifies the success of the replication process. In both cases, contact angles decreases steadily at a constant rate up to around 1.2 μL of droplet sizes. Below a droplet volume of around 1.2 μL, the rate of change in contact angles became much faster, which could be explained by the collapse of the water droplet into the micrometer sized cavities because of the increasing Laplace pressure within the small-diameter droplets with respect to the capillary force that keeps the water droplet stable over the surface [22,23].

4. Conclusions

In this work we demonstrated the first-time use of solvent-free initiated chemical vapor deposition process in biomimetic studies. Conformal nature of iCVD helps to make exact copies of natural surfaces through a two-step replication process. Biomimetic polymer sheet templated from the fresh petal surface of a red rose possessed the same wetting characteristics of the rose surface. By using the same duplication process, many other natural surfaces can be copied into chemically well-defined polymer films or sheets. Different functionalities can be implemented into a single replica film or sheet, through a stacked deposition of polymer layers with different functional groups. iCVD can easily be scaled up for deposition on large or multiple substrates, making the bionic duplication processes feasible in industrial scales.

Acknowledgement

This research was supported by the Scientific and Technological Research Council of Turkey (TUBITAK) (Project No. 110M088).

References

[1] C. Neinhuis, W. Barthlott, Characterization and distribution of water-repellent, self-cleaning plant surfaces, Annals of Botany 79 (1997) 667–677.
[2] R. Blossey, Self-cleaning surfaces – virtual realities, Nature Materials 2 (2003) 301–306.
[3] J. Genzer, A. Marmur, Biological and synthetic self-cleaning surfaces, MRD Bulletin 33 (2008) 742–746.
[4] L. Gao, T.J. McCarthy, The lotus effect explained: two reasons why two length scales of topography are important, Langmuir 22 (2006) 2966–2967.
[5] A. Marmur, The lotus effect: superhydrophobicity and metastability, Langmuir 20 (2004) 3517–3519.
[6] L. Feng, Y. Zhang, J. Xi, Y. Zhu, N. Wang, F. Xia, L. Jiang, Petal effect: a superhydrophobic state with high adhesive force, Langmuir 24 (2008) 4114–4119.
[7] X. Yao, Y. Song, L. Jiang, Applications of bio-inspired special wettable surfaces, Advanced Materials 23 (2011) 719–734.
[8] H.F. Hoefnagels, D. Wu, G. With, W. Ming, Biomimetic superhydrophobic and highly oleophobic cotton textiles, Langmuir 23 (2007) 13158–13163.
[9] G. Cook, P.L. Timms, C.G. Spickermann, Exact replication of biological structures by chemical vapor deposition of silica, Angewandte Chemie International Edition 42 (2003) 557–559.
[10] L. Feng, S. Li, Y. Li, H. Li, L. Zhang, J. Zhai, Y. Song, B. Liu, L. Jiang, D. Zhu, Superhydrophobic surfaces: from natural to artificial, Advanced Materials 14 (2002) 1857–1860.
[11] M. Ma, Y. Mao, M. Gupta, K.K. Gleason, G.C. Rutledge, Superhydrophobic fabrics produced by electrospinning and chemical vapor deposition, Macromolecules 38 (2005) 9742–9748.
[12] K.K.S. Lau, J. Bico, K.B.K. Teo, M. Chhowalla, G.A.J. Amaratunga, W.I. Milne, G.H. McKinley, K.K. Gleason, Superhydrophobic carbon nanotube forests, Nano Letters 3 (2003) 1701–1705.
[13] L. Li, N. Koshizaki, Vertically aligned and ordered hematite hierarchical columnar arrays for applications in field-emission, superhydrophilicity, and photocatalysis, Materials Chemistry 20 (2010) 2972–2978.
[14] D.P. Pulsifer, A. Lakhtakia, R.J.M. Palma, C.G. Pantano, Mass fabrication technique for polymeric replicas of arrays of insect corneas, Bioinspiration and Biomimetics 5 (2010) 1–9.
[15] S. Lee, T.H. Kwon, Mass-producible replication of highly hydrophobic surfaces from plant leaves, Nanotechnology 17 (2006) 3189–3196.
[16] S.H. Baxamusa, K.K. Gleason, Initiated chemical vapor deposition of polymer films on nonplanar substrates, Thin Solid Films 517 (2009) 3536–3538.
[17] A. Asatekin, M.C. Barr, S.H. Baxamusa, K.K.S. Lau, W. Tenhaeff, J. Xu, K.K. Gleason, Designing polymer surfaces via vapor deposition, Materials Today 13 (2010) 26–33.
[18] K. Koch, B. Bhushan, Y.C. Jung, W. Barthlott, Fabrication of artificial lotus leaves and significance of hierarchical structure for superhydrophobicity and low adhesion, Soft Matter 5 (2009) 1386–1393.
[19] A.B.D. Cassie, S. Baxter, Wettability of porous surfaces, Transactions of the Faraday Society 40 (1944) 546–551.
[20] S.A. Kulinich, M. Farzaneh, Effect of contact angle hysteresis on water droplet evaporation from super-hydrophobic surfaces, Applied Surface Science 255 (2009) 4056–4060.
[21] T.A.H. Nguyen, A.V. Nguyen, M.A. Hampton, Z.P. Xu, L. Huang, V. Rudolph, Theoretical and experimental analysis of droplet evaporation on solid surfaces, Chemical Engineering Science 69 (2012) 522–529.
[22] M. Callies, D. Quere, On water repellency, Soft Matter 1 (2005) 55–61.
[23] C. Luo, M. Xiang, X. Liu, H. Wang, Transition from Cassie–Baxter to Wenzel States on microline-formed PDMS surfaces induced by evaporation or pressing of water droplets, Microfluidics and Nanofluidics 10 (2011) 831–842.